

Synthesis, Structural, Spectroscopic, and Magnetic Characterization of Two-Coordinate Cobalt(II) Aryloxides with Bent or Linear Coordination

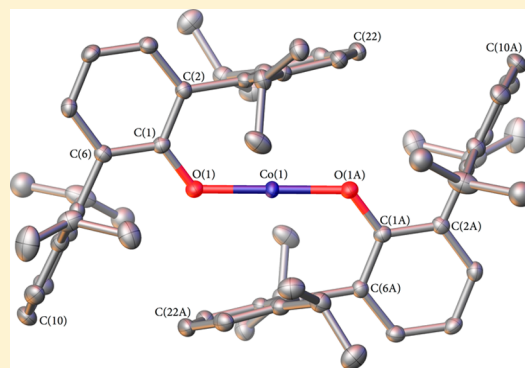
Aimee M. Bryan,[†] Gary J. Long,^{*,‡} Fernande Grandjean,[‡] and Philip P. Power^{*,†}

[†]Department of Chemistry, University of California, Davis, One Shields Avenue, Davis, California 95616, United States

[‡]Department of Chemistry, Missouri University of Science and Technology, University of Missouri, Rolla, Missouri 65409, United States

S Supporting Information

ABSTRACT: Treatment of the cobalt(II) amide, $[\text{Co}\{\text{N}(\text{SiMe}_3)_2\}_2]_2$, with four equivalents of the sterically crowded terphenyl phenols, $\text{HOAr}^{\text{Me}_6}$ ($\text{Ar}^{\text{Me}_6} = \text{C}_6\text{H}_3\text{-}2,6(\text{C}_6\text{H}_2\text{-}2,4,6\text{-Me}_3)_2$) or $\text{HOAr}^{\text{iPr}_4}$ ($\text{Ar}^{\text{iPr}_4} = \text{C}_6\text{H}_3\text{-}2,6(\text{C}_6\text{H}_3\text{-}2,6\text{-Pr}^i)_2$), produced the first well-characterized, monomeric two-coordinate cobalt(II) bisaryloxides, $\text{Co}(\text{OAr}^{\text{Me}_6})_2$ (**1**) and $\text{Co}(\text{OAr}^{\text{iPr}_4})_2$ (**2a** and **2b**), as red solids in good yields with elimination of $\text{HN}(\text{SiMe}_3)_2$. The compounds were characterized by electronic spectroscopy, X-ray crystallography, and direct current magnetization measurements. The O–Co–O interligand angles in **2a** and **2b** are 180° , whereas the O–Co–O angle in **1** is bent at $130.12(8)^\circ$ and its cobalt(II) ion has a highly distorted pseudotetrahedral geometry with close interactions to the *ipso*-carbons of the two flanking aryl rings. The Co–O distances in **1**, **2a**, and **2b** are 1.858(2), 1.841(1), and 1.836(2) Å respectively. Structural refinement revealed that **1**, **2a**, and **2b** have different fractional occupations of the cobalt site in their crystal structures: **1**, 95.0%, **2a**, 93.5%, and **2b**, 84.6%. Correction of the magnetic data for the different cobalt(II) occupancies showed that the magnetization of **2a** and **2b** was virtually identical. The effective magnetic moments for **1**, **2a**, and **2b**, 5.646(5), 5.754(5), and 5.636(3) μ_{B} respectively, were indicative of significant spin–orbit coupling. The differences in magnetic properties between **1** and **2a/2b** are attributed to their different cobalt coordination geometries.



INTRODUCTION

Interest in open shell (d^1 – d^9) two-coordinate transition metal complexes continues to grow because of their unique chemical, structural, and magnetic properties.^{1,2} The major challenge in their isolation and study is the prevention of aggregation and/or decomposition via disproportionation. In addition, the complexes are generally very air and moisture sensitive due to their unsaturated coordination.^{1,2} The most common method of stabilizing such complexes is with the use of sterically large ligands.³ Even so, complexes with strictly linear coordination in the solid state remain scarce and constitute a small fraction of known two-coordinate species.^{1,2} Two- or three-coordinate complexes, especially those of iron(II) and cobalt(II), are important because they may have orbital angular momentum and effective magnetic moments that approach free ion values.^{4–13} Furthermore, it has been shown that in the two-coordinate complexes deviations from linear geometry (i.e., bending) result in a lowering of the magnetic moment due to quenching of the orbital angular momentum.^{4,5,8} Large spin–orbit coupling and magnetic anisotropy are thought to be major contributors to a compound's axial zero field splitting term (D) and thereby its spin-reversal barrier (U) where $U = S^2D$ for non-Kramer integer S or $U = (S^2 - 1/4)D$ for Kramer half-

integer S values.^{14–16} Large negative D values indicate the possible presence of magnetic hysteresis and therefore single molecule magnet behavior.^{5,15,17} Single molecule magnets are currently of interest because of their potential applications in magnetic memory,¹⁸ high-density information storage,¹⁸ and quantum computing technologies.^{19–21} The majority of currently known stable, two-coordinate linear complexes are derivatives of amido ligands,^{4,8,22–26} although several alkyl^{6,7,27–32} and thiolato^{28,33,34} derivatives are known. A small number of diaryl compounds also exist, but none has a linear metal coordination.³⁵ In contrast, two-coordinate derivatives of alkoxide or aryloxide ligands are exceedingly rare. The only known monomeric two-coordinate first-row transition metal aryloxide complexes are the strictly linear iron(II) derivative, $\text{Fe}(\text{OAr}^{\text{iPr}_4})_2$ ($\text{Ar}^{\text{iPr}_4} = \text{C}_6\text{H}_3\text{-}2,6(\text{C}_6\text{H}_3\text{-}2,6\text{-Pr}^i)_2$),³⁶ synthesized by the addition of an excess of O_2 to $\text{Fe}(\text{Ar}^{\text{iPr}_4})_2$ at -100°C , and the bent ($\text{O–Fe–O} = 175.43(15)^\circ$ and $171.15(11)^\circ$) iron(II) derivatives $\text{Fe}(\text{OAr}^{\text{AdR}})_2$ ($\text{Ar}^{\text{AdR}} = \text{C}_6\text{H}_3\text{-}2,6(1\text{-Ad})_2\text{-}4\text{-R}$; Ad = adamantyl, R = Me, Prⁱ),³⁷ obtained by adding four equivalents of HOAr^{AdR} to $[\text{Fe}\{\text{N}$

Received: December 18, 2013

Published: February 17, 2014

(SiMe₃)₂}]₂.³⁷ To date no two-coordinate aryl or alkyloxo cobalt(II) derivatives have been well-characterized. However, several three-coordinate cobalt(II) alkoxides and aryloxo complexes, such as [Co(Cl)(OC-*t*-Bu)₃·Li(THF)₃][Li(THF)_{4.5}],³⁸ [Co{N(SiMe₃)₂}(OC-*t*-Bu)₂}]₂,³⁸ and [Li{Co(N(SiMe₃)₂)(OC-*t*-Bu)₂}]₂,³⁸ which have distorted trigonal-planar cobalt(II) geometry, are known. In addition, the more recently reported [Na(THF)₆][Co(OAr)₃] (OAr = 2,4,6-tri-*tert*-butylphenoxo)³⁹ has a regular trigonal planar geometry at the cobalt(II) anion. The first neutral three-coordinate cobalt(II) alkyloxides to be characterized were the dimers [Co{OC(C₆H₁₁)₃}]₂·CH₃OH·(1/2)C₆H₁₂·THF and [Co(OCPh₃)₂]₂·*n*-C₆H₁₄ which have trigonal planar coordination at their cobalt ions.⁴⁰ Another low-coordinate cobalt(II) aryloxo species is {K(18-crown-6)}[Co(OC₄F₉)₃], which was structurally characterized as its pseudo three-coordinate salt {K(18-crown-6)}[Co(OC₄F₉)₃](THF).⁴¹ Herein, we report the first monomeric neutral two-coordinate cobalt(II) aryloxo species, one of which features a strictly linear cobalt coordination geometry, whereas the other has a bent O–Co–O geometry with additional interactions between the *ipso*-carbons of the flanking aryl rings of the terphenyl oxygen substituents. In addition, we report that careful manipulation of the synthetic conditions can produce varying occupancies of the cobalt(II) site.

EXPERIMENTAL SECTION

All manipulations were performed with the use of modified Schlenk techniques or in a Vacuum Atmospheres drybox under N₂ or argon. Solvents were dried and collected using a Grubbs-type Glass Contour solvent purification system⁴² and degassed by using the freeze–pump–thaw method. All physical measurements were obtained under strictly anaerobic and anhydrous conditions. IR spectra were recorded as Nujol mulls between CsI plates on a Perkin-Elmer 1430 spectrophotometer. UV–visible spectra were recorded as dilute toluene solutions in 3.5 mL quartz cuvettes using an Olis 17 modernized Cary 14 UV/vis/NIR spectrophotometer. Melting points were determined on a MEL-TEMP II apparatus using glass capillaries sealed with vacuum grease and are uncorrected. Unless otherwise stated, all materials were obtained from commercial sources and used as received. HOAr^{Me₆},⁴³ HOAr^{iPr₄},⁴⁴ and [Co{N(SiMe₃)₂}]₂⁴⁵ were prepared according to literature procedures.

Co(OAr^{Me₆})₂ (1). [Co{N(SiMe₃)₂}]₂ (0.63 g, 1.7 mmol), powdered HOAr^{Me₆} (2.2 g, 6.6 mmol), and a magnetic stir bar were added to a Schlenk flask. The flask was heated in an oil bath to ca. 85 °C, at which temperature the brown cobalt silylamide began to melt to a green liquid. Immediately, the slurry became red with formation of a white vapor. The flask was briefly placed under reduced pressure to remove the eliminated HN(SiMe₃)₂. This process was repeated until the white vapor ceased to form. The dark red solids were then extracted with ca. 30 mL of hot toluene. The volume of the dark red solution was halved under reduced pressure, and upon standing at 25 °C for 12 h, **1** was obtained as dark red, blocklike crystals. Yield: 1.84 g (78.0%). Mp: >250 °C. UV–vis (toluene, nm [ε, M⁻¹ cm⁻¹]): 245 [2030], 256 [1380], 283 [6400], 419 [250], 594 [40], 643 [40], 808 [150], 1522 [30]. IR in Nujol mull (cm⁻¹) in CsI plates: 3170, 2900, 2730, 2670, 1600, 1580, 1450, 1370, 1295, 1260, 1150, 1065, 950, 890, 850, 800, 770, 720, 660, 615, 535, 440, 390, 350, 300. Anal. Calcd for C₄₈H₅₀Co_{0.95}O₂ (**1**): C, 80.64%; H, 7.05%. Found: C, 80.57%; H, 7.18%.

Co(OAr^{iPr₄})₂ (2a). [Co{N(SiMe₃)₂}]₂ (0.95 g, 2.5 mmol), powdered HOAr^{iPr₄} (4.2 g, 10.1 mmol), and a stir bar were added to a Schlenk flask. The flask was heated in an oil bath to ca. 85 °C, at which temperature the brown cobalt(II) silylamide began to melt to a green liquid. Immediately, the slurry became red with formation of a white vapor. The flask was briefly placed under reduced pressure to remove the eliminated HN(SiMe₃)₂. This process was repeated until

the white vapor ceased to form. Vacuum was then applied, and the oil bath temperature was raised to ca. 165 °C for 2 h in order to sublime excess HOAr^{iPr₄} away from the Co(OAr^{iPr₄})₂ product. After heating, the red powder remaining at the bottom of the flask was extracted with ca. 50 mL of hot toluene. The dark red solution was concentrated under reduced pressure, which upon standing at 25 °C overnight afforded crystals of **2a** as red blocks. Yield: 2.59 g (58.5%). Mp: 298–301 °C. UV–vis (toluene, nm [ε, M⁻¹ cm⁻¹]): 245 [210], 283 [3230], 458 [40], 600 [7], 654 [10], 808 [50], 1662 [20]. IR in Nujol mull (cm⁻¹) in CsI plates: 3140, 2900, 2720, 2660, 1570, 1450, 1370, 1290, 1240, 1145, 1065, 940, 880, 850, 795, 780, 745, 715, 660, 600, 550, 430, 380. Anal. Calcd. for C₆₀H₇₄Co_{0.935}O₂ (**2a**): C, 81.68%; H, 8.45%. Found: C, 81.64%; H, 8.47%.

Co(OAr^{iPr₄})₂ (2b). [Co{N(SiMe₃)₂}]₂ (0.20 g, 0.50 mmol), powdered HOAr^{iPr₄} (0.83 g, 2.0 mmol), and a stir bar were added to a Schlenk flask. The flask was heated in an oil bath to ca. 85 °C, at which temperature the brown cobalt(II) silylamide began to melt to a green liquid. Immediately, the slurry became red with formation of a white vapor. The flask was briefly placed under reduced pressure to remove the eliminated HN(SiMe₃)₂. This process was repeated until the white vapor ceased to form. The red solids were then extracted with ca. 20 mL of hot toluene. The dark red solution was concentrated under reduced pressure. The solution was then placed in a –18 °C freezer overnight, which afforded X-ray diffraction quality crystals of **2b** as red blocks.

X-ray Crystallography. Crystals for X-ray diffraction studies were removed from the Schlenk tube under a stream of nitrogen and immediately covered with hydrocarbon oil (Paratone-N). A suitable crystal was selected, attached to a mounting pin, and quickly placed in a low-temperature stream of nitrogen at ca. 90 K.⁴⁶ Data for compounds **1**, **2a**, and **2b** were obtained on an APEX-II DUO or SMART APEX-II diffractometer using Mo Kα radiation (λ = 0.71073 Å) in conjunction with a CCD detector. A multiscan absorption correction was applied with the program SADABS.⁴⁷ The structures were solved by direct methods and refined with the SHELXTL (2013) software package. The thermal ellipsoid plots were drawn using OLEX2 software.^{48,49} Refinement was by full-matrix least-squares procedures with all carbon-bound hydrogen atoms included in calculated positions and treated as riding atoms. This refinement indicated that the cobalt(II) occupancy for **1** was 0.950(8), for **2a**, 0.935(3), and for **2b**, 0.846(2). A summary of crystallographic and data collection parameters for **1**, **2a**, and **2b** is given in Table 1.

Magnetic Studies. The powdered samples of **1**, **2a**, and **2b** used for magnetic measurements were sealed under vacuum in 6 mm outer and 4 mm inner diameter quartz tubes with a thin shelf, and the sample moment was measured using a Quantum Design MPMSXL7 superconducting quantum interference magnetometer. To prevent crystallite reorientation by the applied field, each sample was anchored with eicosane. For each compound the sample was zero-field cooled to 2 K and the moment was measured upon warming to 300 K in an applied field of 0.01 T. In order to ensure thermal equilibrium between the powdered sample sealed under vacuum in the quartz tube and the temperature sensor, the moment was measured at a given sensor temperature until a constant value moment was observed; ca. 14 h were required for the measurements between 2 and 300 K. The measured long moments were corrected for both the presence of diamagnetic eicosane and the diamagnetic free ligand, HOAr^{Me₆} or HOAr^{iPr₄}; no quartz tube correction was necessary because the quartz tube extended equally above and below the sample by ca. 5 cm. Diamagnetic corrections of –0.000468, –0.000611, –0.000450, and –0.000605 emu/mol, obtained from tables of Pascal's constants, have been applied to the molar susceptibility of **1**, **2**, HOAr^{Me₆}, and HOAr^{iPr₄}, respectively.⁵⁰ Due to the partial occupancy of the cobalt(II) site in **1**, **2a**, and **2b**, the measured magnetic susceptibility is the sum of two contributions, one from the fully occupied **1** or **2** and one from HOAr^{Me₆} or HOAr^{iPr₄}; these contributions are weighted according to the partial cobalt(II) occupancy as given above. Hence, the magnetic susceptibility of **1**, **2a**, and **2b** are reported per mole of fully occupied **1** or **2**. Statistical fitting errors are estimated below; the actual errors may be as much as twice as large. The 5 K magnetizations, *M*, of **1**, **2a**, and

Table 1. Selected Crystallographic and Data Collection Parameters for Complexes **1**, **2a**, and **2b**

	Co(OAr ^{Me₆}) ₂ (1)	Co(OAr ^{iPr₄}) ₂ (2a)	Co(OAr ^{iPr₄}) ₂ (2b)
formula	C ₄₈ H ₅₀ Co _{0.95} O ₂	C ₆₀ H ₇₄ Co _{0.935} O ₂	C ₆₀ H ₇₄ Co _{0.846} O ₂
fw, g/mol	714.85	882.26	877.03
color, habit	red, block	red, block	red, block
cryst syst	triclinic	monoclinic	monoclinic
space group	$P\bar{1}$	$P2_1/n$	$P2_1/n$
<i>a</i> , Å	9.136(1)	10.7205(7)	10.7365(8)
<i>b</i> , Å	11.570(2)	20.214(1)	20.206(2)
<i>c</i> , Å	19.045(3)	11.2077(7)	11.1732(9)
α , deg	99.748(2)	90	90
β , deg	95.692(2)	90.3380(9)	90.411(1)
γ , deg	105.565(2)	90	90
<i>V</i> , Å ³	1888.9(5)	2428.7(3)	2423.9(3)
<i>Z</i>	2	2	2
cryst dimens, mm	0.72 × 0.31 × 0.18	0.94 × 0.89 × 0.76	0.23 × 0.23 × 0.14
<i>T</i> , K	90	90	90
<i>d</i> _{calc} , g/cm ³	1.257	1.206	1.202
abs coeff μ , mm ⁻¹	0.472	0.375	0.346
θ range, deg	2.734–28.921	2.150–27.481	2.016–27.482
<i>R</i> (int)	0.0585	0.0258	0.0629
obsd reflns [<i>I</i> > 2 σ (<i>I</i>)]	5333	4849	4275
data/restraints/params	9020/0/473	5556/4/296	5547/4/296
<i>R</i> ₁ , obsd reflns	0.0551	0.0383	0.0501

2b were subsequently measured in a 0 to 7 T applied field; no hysteresis was observed upon returning the applied field to zero. No eicosane, free-ligand, or compound diamagnetic corrections have been applied to the magnetization results because their contributions are essentially trivial at 5 K.

RESULTS AND DISCUSSION

Synthesis. Our goal was to synthesize monomeric, two-coordinate cobalt(II) bis(aryloxides) in good yields by a simple and convenient route. After several attempts to synthesize the desired products using a salt metathesis approach involving treatment of CoCl₂ with two equivalents of lithium aryloxides were unsuccessful, we investigated the reaction of the terphenols HOAr^{Me₆} and HOAr^{iPr₄} with [Co{N(SiMe₃)₂}₂]₂ for the synthesis of the bis(aryloxide) complexes **1**, **2a**, and **2b**. These were prepared by melting [Co{N(SiMe₃)₂}₂]₂ with four equivalents of finely ground phenol under positive N₂ atmosphere until a color change was observed and eliminated HN(SiMe₃)₂ formed as a white vapor. The reaction was facilitated by the relatively low melting point of [Co{N(SiMe₃)₂}₂]₂ (89–90 °C)⁴⁵ and the volatility of HN(SiMe₃)₂. As soon as the brown silylamide melted, the slurry immediately became a dark red color. Over several minutes intermittent vacuum was applied during heating to remove the eliminated vapor. The removal of HN(SiMe₃)₂ promoted completeness of the reaction, however, it was found that the use of excessive heat under reduced pressure could also result in the loss of [Co{N(SiMe₃)₂}₂]₂ as a dark green vapor.⁴⁵ The crude red product was then extracted with hot toluene, concentrated, and left to stand undisturbed overnight at 25 °C to yield dark red crystals that were suitable for X-ray analysis. X-ray crystallography showed that the product **2b** had a cobalt(II) occupancy of 84.6(2)%; however, a second synthesis of the OAr^{iPr₄} derivative under similar conditions but where the resulting

crude product was heated to ca. 165 °C at 5 × 10⁻² Torr for 2 h resulted in a dark red residue and colorless crystals which had sublimed on the upper walls of the flask. The red solid was then recrystallized from hot toluene, which afforded compound **2a** with a cobalt(II) occupancy of 93.5(3)% as indicated by X-ray diffraction. ¹H NMR spectroscopy and a melting point measurement confirmed that the sublimed colorless crystals were pure HOAr^{iPr₄}.⁴⁴ We conclude that the steric bulk of Ar^{iPr₄} may prevent completion of the reaction thereby permitting unreacted HOAr^{iPr₄} to be incorporated in the crystal structure of **2**. Fractional occupation of free ligand in the crystal structure was further demonstrated by recrystallizing one equivalent of **2a** from a hot toluene solution which contained ca. 5.5 equivalents of excess HOAr^{iPr₄}. The cobalt occupancy of crystals grown from this solution was determined to be ca. 55% by X-ray diffraction. Fractional occupation by HOAr^{iPr₄} and the cobalt(II) bis(aryloxide) compound is reasonable because the unit cells of **2a** and **2b** are nearly identical to that of HOAr^{iPr₄} (monoclinic, $P2_1/n$, *Z* = 4; at 90 K, *a* = 10.858(1) Å, *b* = 20.831(2) Å, *c* = 11.1785(8) Å, β = 94.474(7)°).⁴⁴ The bent geometry cobalt(II) species, Co(OAr^{Me₆})₂ (**1**), was synthesized in a like manner to **2a** and **2b**, but it was found that crystallization from toluene of the crude product without further heating produced dark red crystals of **1** with 95.0(8)% occupancy of the cobalt(II) site. We conclude that the smaller steric bulk of the HOAr^{Me₆} ligand enables more effective proton transfer than that of the larger HOAr^{iPr₄}. This difference, along with the fact that HOAr^{Me₆} and **1** have different unit cell dimensions, favors a more complete reaction as reflected in the higher yield of **1** (76%) versus **2a** (58%) and the higher cobalt(II) occupancy in **1** without the requirement of more forceful reaction conditions. Furthermore, in support of these crystallographic results, the magnetic data correlate with the partial occupancy of the cobalt(II) sites.

Structures. The structures of **1** and **2a** are illustrated in Figures 1 and 2, and selected bond lengths and angles of **1**, **2a**, and **2b** are listed in Table 2. The bent structure of **1**, in contrast to the linear structures of **2a** and **2b**, is primarily a result of the smaller size of the OAr^{Me₆} ligand in comparison to OAr^{iPr₄}, which permits secondary Co–C interaction between the relatively electron-poor cobalt(II) and electron-rich flanking

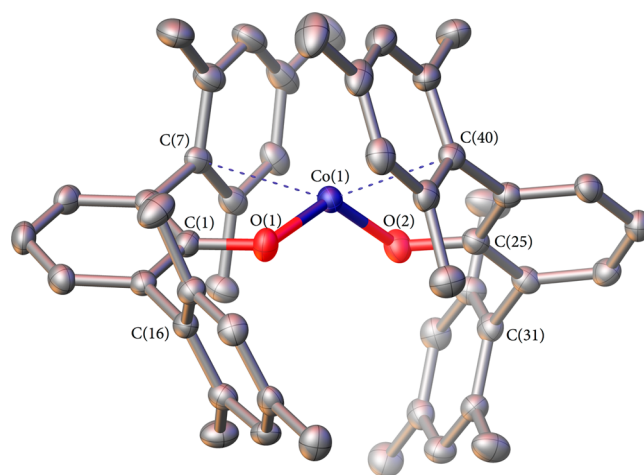


Figure 1. Thermal ellipsoid (50%) drawing of Co(OAr^{Me₆})₂ (**1**). Dashed lines indicate closest cobalt(II) aryl ring carbon interactions. H atoms are not shown for clarity. Selected bond lengths and angles are given in Table 2.

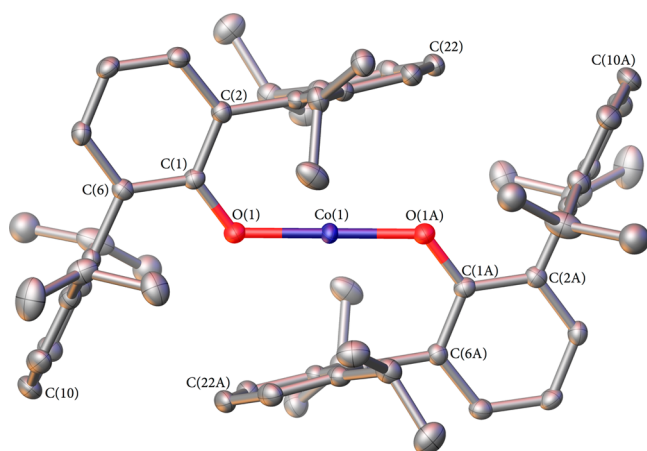


Figure 2. Thermal ellipsoid (50%) drawing of $\text{Co}(\text{OAr}^{\text{iPr}_4})_2$ (**2a**). H atoms and disorder are not shown for clarity. Selected bond lengths and angles are given in Table 2

aryl rings, without undue steric pressure. In contrast, the linear cobalt geometry in **2a** and **2b** is sustained by the larger size of the Ar^{iPr_4} terphenyl groups, where bending and closer approach of these groups are disfavored for steric reasons. The Co–O distances in **1** are 1.858(2) and 1.859(2) Å, in **2a** the Co–O distance is 1.841(1) Å, and in **2b** it is 1.836(2) Å. These bond lengths are comparable to the Fe–O distance of 1.847(1) Å in $\text{Fe}(\text{OAr}^{\text{iPr}_4})_2$.³⁶ They are also comparable to the Co–N bond lengths, 1.827(8) Å and 1.865(2) Å, in the related isoelectronic amido derivatives, $\text{Co}\{\text{N}(\text{H})\text{Ar}^{\text{Me}_6}\}_2$ and $\text{Co}\{\text{N}(\text{H})\text{Ar}^{\text{iPr}_6}\}_2$, respectively.⁴ In contrast, the distances are shorter than the average Co–N bond length, 1.901(3) Å, in the two-coordinate complex $[\text{Co}\{\text{N}(\text{SiMePh}_2)_2\}_2]$.⁵¹ Interestingly, the Co–O distances in **1** are slightly longer than those of its linear counterparts, **2a** and **2b**, whereas the Co–N distances of **1**'s amide congener, $\text{Co}\{\text{N}(\text{H})\text{Ar}^{\text{Me}_6}\}_2$,⁴ 1.845(8) and 1.827(8) Å, are shorter than those in its bulkier counterpart, $\text{Co}\{\text{N}(\text{H})\text{Ar}^{\text{iPr}_6}\}_2$ (1.865(2) Å, see Table 2).⁴ The O–Co–O angle of 130.12(8)° in **1** is narrower than that of 144.1(4)° in $\text{Co}\{\text{N}(\text{H})\text{Ar}^{\text{Me}_6}\}_2$ ⁴ and 140.9(2)° in $\text{Fe}\{\text{N}(\text{H})\text{Ar}^{\text{Me}_6}\}_2$.⁸ These differences could be due to the stronger cobalt(II) *ipso*-carbon interaction, as indicated by the shorter Co–C distances of 2.435 Å (average) for **1**, in comparison to those of the amido congeners, $\text{Co}\{\text{N}(\text{H})\text{Ar}^{\text{Me}_6}\}_2$ at 2.56 Å (average)⁴ and $\text{Fe}\{\text{N}(\text{H})\text{Ar}^{\text{Me}_6}\}_2$ at 2.64 Å (average).⁸ The narrower O–Co–O angle and shorter cobalt(II) *ipso*-carbon interactions afford what is effectively a highly distorted pseudotetrahedral, four-coordinate, cobalt(II) ion which leads to longer Co–O bonds. The O–Co–O angles of **2a** and **2b** are required to be 180° by the position of cobalt(II) at the crystallographic inversion center. The same is also true for the metal ions in $\text{Co}\{\text{N}(\text{H})\text{Ar}^{\text{iPr}_6}\}_2$,⁴ $\text{Fe}\{\text{N}(\text{H})\text{Ar}^{\text{iPr}_6}\}_2$,⁸ and $\text{Fe}(\text{OAr}^{\text{iPr}_4})_2$.³⁶ Ster-

ic crowding has been cited as the reason for the linear geometry, but similar nonlinear compounds with high steric crowding such as $[\text{Co}\{\text{N}(\text{SiMePh}_2)_2\}_2]$ ⁵¹ and $\text{Fe}(\text{OAr}^{\text{AdR}})_2$ ³⁷ suggest that other factors are probably involved.^{52,53} It is possible that dispersion forces involving interactions between C–H moieties of the isopropyl groups from the two terphenyl substituents are strong enough to stabilize linear geometry at the metal, as observed in **2a**, **2b**, and $\text{Fe}(\text{OAr}^{\text{iPr}_4})_2$ ³⁶ and in $\text{M}\{\text{N}(\text{H})\text{Ar}^{\text{iPr}_6}\}_2$, where M = V,²² Cr,²⁴ Mn,⁵⁴ Fe,⁸ Co,⁴ and Ni.⁴ The effects of dispersion forces produced by the less ramified Ar^{Me_6} substructure may be insufficient to induce linear geometry, and the lower steric requirement of Ar^{Me_6} in comparison to Ar^{iPr_4} or Ar^{iPr_6} permits significant bending of the divalent metal geometries to form a pseudotetrahedral arrangement with the *ipso*-carbons as demonstrated in the compounds **1**, $\text{Co}\{\text{N}(\text{H})\text{Ar}^{\text{Me}_6}\}_2$,⁴ and $\text{Fe}\{\text{N}(\text{H})\text{Ar}^{\text{Me}_6}\}_2$.⁸ Computational and synthetic studies are underway to further understand the effects and implications of dispersion on two- and three-coordinate mononuclear transition metal compounds.

Spectroscopy. A cobalt(II) free ion has a ground state of $^4\text{F}_{9/2}$. In an idealized $D_{\infty h}$ ligand field with orbital energy ordering of $d_z^2 < d_{xy} \sim d_{x^2-y^2} < d_{xz} \sim d_{yz}$, the $^4\text{F}_{9/2}$ ground state splits into the $^4\Sigma_g^+$, $^4\Delta_g$, $^4\Pi_g$ and $^4\Phi_g$ electronic states. Thus, at least three bands in the UV–vis spectra are expected with more bands possible because of transitions to the $^4\Pi_g$ (P) excited states. The linear compound, **2a**, displays seven absorptions with the four longer wavelength bands having low intensities indicating that they are d–d transitions (nm [ϵ , $\text{M}^{-1} \text{cm}^{-1}$]: 1662 [20], 808 [50], 654 [10], 600 [7]). In the lower ligand field symmetry of the bent species, **1**, more than three bands are expected because of the lifting of the degeneracy of the states. Compound **1** has four observable bands at 1522 [30], 808 [150], 643 [40], 594 [40] nm [ϵ , $\text{M}^{-1} \text{cm}^{-1}$]; but it is possible that other absorptions exist but are too weak to be visible. The absorptions at 458 [40] for **2a** and 419 [250] for **1**, together with the long tail of the more intense absorptions at shorter wavelengths, are consistent with the compounds' red colors. The higher intensity absorptions for both **1** (283 [6400], 256 [1380], 245 [2030]) and **2a** (283 [3230], 245 [210]) are likely due either to ligand to cobalt(II) electron transfer bands from the lone pairs on the oxygen to the cobalt(II) d-orbitals or π – π^* transitions in the ligand. Unfortunately, near IR spectra for analogous compounds such as $\text{Fe}(\text{OAr}^{\text{Pr}_4})_2$ and $\text{Fe}(\text{OAr}^{\text{AdR}})_2$ have not been measured; therefore comparisons cannot be made at present. Alternatively, the $\nu(\text{M}–\text{O})$ bands for **1** at 390 cm^{-1} and **2a** at 380 cm^{-1} are comparable to the amide analogues at 385 cm^{-1} for $\text{Co}\{\text{N}(\text{H})\text{Ar}^{\text{Me}_6}\}_2$ ⁴ and 380 cm^{-1} for $\text{Co}\{\text{N}(\text{H})\text{Ar}^{\text{iPr}_6}\}_2$.⁴ The characteristic $\nu(\text{H}–\text{O})$ band at 3540 cm^{-1} for $\text{HOAr}^{\text{Me}_6}$ ⁴³ and 3530 cm^{-1} for $\text{HOAr}^{\text{iPr}_4}$ ⁴⁴ does not appear in the IR spectra of **1** and **2a** respectively, demonstrating that free ligand either is

Table 2. Selected Interatomic Distances (Å) and Angles (deg) for Compounds **1**, **2a**, and **2b** and their Amido Analogues $\text{Co}\{\text{N}(\text{H})\text{Ar}^{\text{Me}_6}\}_2$ and $\text{Co}\{\text{N}(\text{H})\text{Ar}^{\text{iPr}_6}\}_2$

	$\text{Co}(\text{OAr}^{\text{Me}_6})_2$ (1)	$\text{Co}(\text{OAr}^{\text{iPr}_4})_2$ (2a)	$\text{Co}(\text{OAr}^{\text{iPr}_4})_2$ (2b)	$\text{Co}\{\text{N}(\text{H})\text{Ar}^{\text{Me}_6}\}_2$ ⁴	$\text{Co}\{\text{N}(\text{H})\text{Ar}^{\text{iPr}_6}\}_2$ ⁴
Co–L(1)	1.858(2)	1.841(1)	1.836(2)	1.827(8)	1.865(2)
Co–L(2)	1.859(2)			1.845(8)	
L(1)–Co–L(1A,2)	130.12(8)	180	180	144.1(4)	180
<i>ipso</i> -C–Co	2.387(2) ^a , 2.482(2) ^b	2.680(1)	2.696(2)	2.56 (av)	2.61 (av)

^aC(7)–Co. ^bC(40)–Co.

not present or is present in such a small quantity that it is not detectable by normal IR spectroscopy. The $\nu(\text{H}-\text{O})$ band of $\text{HOAr}^{\text{iPr}_4}$ is visible in the spectra of **2a** doped with excess ligand and recrystallized as mentioned in the synthesis section (see also Figure S5 in the Supporting Information). Figure S5 in the Supporting Information clearly displays an overlap of free ligand bands with the characteristic bands of pure $\text{Co}(\text{OAr}^{\text{iPr}_4})_2$.

Magnetism. The magnetic properties of **1**, **2a**, and **2b** have been measured, after zero-field cooling, upon warming from 2 to 300 K in a 0.01 T applied magnetic field. The results in terms of $\chi_{\text{M}}T$ are shown in Figures 3 and 4. As would be

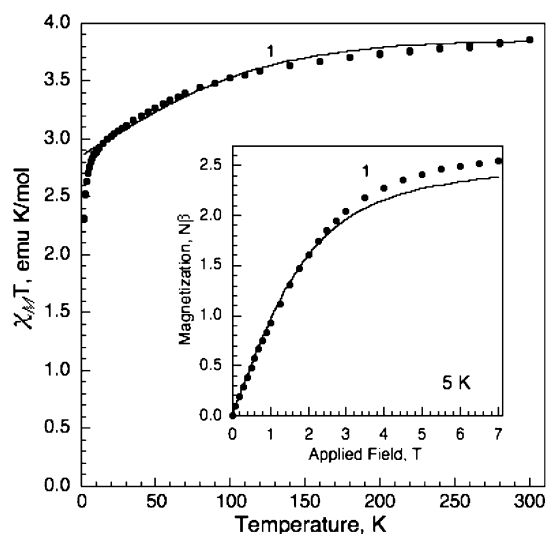


Figure 3. The temperature dependence of $\chi_{\text{M}}T$ obtained at 0.01 T for **1**, points, and a fit line obtained between 2 and 300 K, for cobalt(II) with $S = 3/2$, $L = 2$, and the parameters given in Table 3. Inset: the 5 K magnetization, M , of **1** and its fit with the parameters given in Table 3.

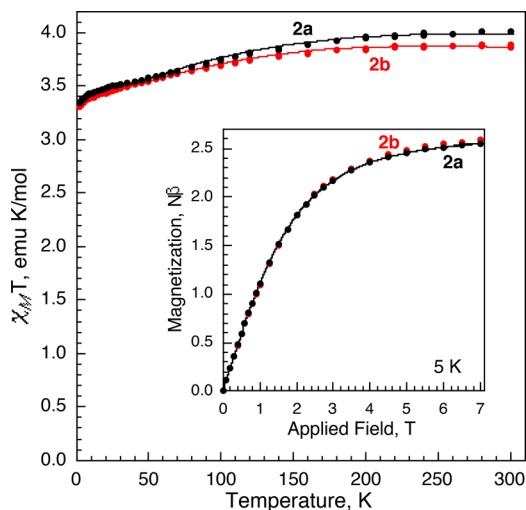


Figure 4. The temperature dependence of $\chi_{\text{M}}T$ obtained at 0.01 T for **2a**, black points, and **2b**, red points, and a fit, black and red lines, obtained between 2 and 300 K, for cobalt(II) with $S = 3/2$, $L = 2$, and the parameters given in Table 3. Inset: the 5 K magnetization, M , of **2a** and **2b** and their fit with the parameters given in Table 3. Note that the calculated fits for **2a** and **2b** are virtually identical and overlap.

expected for these magnetically dilute complexes, $1/\chi_{\text{M}}$ is essentially linear between 50 and 300 K and Curie–Weiss law fits over this temperature range yield the parameters at the top

of Table 3. In Figures 3, 4, and Table 3, it should be noted that the results given correspond to what would be observed if the

Table 3. Magnetic Properties^a of the Complexes **1, **2a**, and **2b****

	$\text{Co}(\text{OAr}^{\text{Me}_6})_2$ (1)	$\text{Co}(\text{OAr}^{\text{iPr}_4})_2$ (2a)	$\text{Co}(\text{OAr}^{\text{iPr}_4})_2$ (2b)
fractional cobalt(II) occupancy ^b	0.950(8)	0.935(3)	0.846(2)
50–300 K Curie–Weiss law fit			
θ , deg	−12.6(3)	−9.7(3)	−6.8(2)
C , emu K/mol	3.984(3)	4.140(3)	3.972(4)
μ_{eff} , μ_{B}	5.646(5)	5.754(5)	5.636(3)
g for $S = 3/2$	2.915(3)	2.971(3)	2.910(1)
2–300 K fit of $\chi_{\text{M}}T$ and 5 K magnetization best fit			
B_2^0 , cm^{-1}	−207(2)	−190(2)	−206(2)
B_2^2 , cm^{-1}	$\pm 79(2)$		
λ , cm^{-1}	−132(5)	−201(2)	−204(2)
g_z	1.9(1)	2.12(1)	2.04(1)
$g_x = g_y$	2.4(1)	2.11(1)	2.12(1)
2–300 K fit of $\chi_{\text{M}}T$ and 5 K magnetization			
B_2^0 , cm^{-1}	−196(2)	−205(2)	−215(2)
B_2^2 , cm^{-1}	$\pm 79(2)$		
λ , cm^{-1} (constrained)	−171.5	−171.5	−171.5
g_z	1.9(1)	2.12(1)	2.05(1)
$g_x = g_y$	2.4(1)	2.12(1)	2.11(1)

^aThe magnetic properties correspond to what would be observed if the cobalt(II) sites in **1**, **2a**, and **2b** were fully occupied. ^bThe occupancy values used to obtain the equivalent fully occupied magnetic properties are given.

cobalt(II) sites in **1**, **2a**, and **2b** were fully occupied. The partial cobalt(II) occupancies given in this table have been used to determine the amount of the moment in emu of the diamagnetic ligand that has been subtracted from the observed moment. The resulting parameters are consistent with cobalt(II) cations with $S = 3/2$ that have a significant orbital contribution to their magnetic moments. The deviation from Curie–Weiss law behavior below 50 K is indicative of the presence of either zero-field splitting and/or spin–orbit coupling of the electronic ground state of the cobalt(II) cations in **1**, **2a**, and **2b**. Initial studies indicated that an analysis in terms of zero-field splitting in the absence of spin–orbit coupling led to very poor fits with unacceptable parameters. As a result, the $\chi_{\text{M}}T$ observed for **1**, **2a**, and **2b** between 2 and 300 K and the corresponding 5 K magnetization have been fitted simultaneously with the PHI code⁵⁵ in terms of the crystal-field parameters, B_2^0 and B_2^2 , the spin–orbit coupling parameter, λ , g_z , and, if called for, $g_x = g_y$ and, when needed, a second order Zeeman contribution, $N\alpha$, to the molar magnetic susceptibility. The results of these fits are shown as the solid lines in Figures 3 and 4; the corresponding best fit parameters for $S = 3/2$ and $L = 2$ are given in the center of Table 3. These figures reveal excellent agreement between the calculated and observed $\chi_{\text{M}}T$ for compounds **1**, **2a**, and **2b** and the 5 K magnetization for **2a** and **2b** but somewhat poorer agreement for the 5 K magnetization of **1**. This poorer agreement may be an indication of some texture in the sample used for the magnetic measurements. Unexpectedly, the value of the spin–orbit coupling constant, λ , when adjusted to obtain the best fits, is

found to be different from the $\lambda = -171.5 \text{ cm}^{-1}$ value found for the cobalt(II) free ion. As a consequence, $\chi_{\text{M}}T$ and the 5 K magnetization have also been simultaneously fitted with λ constrained to the free-ion value; the resulting fits, although having a slightly higher residual, are virtually identical to the best fits shown in Figures 3 and 4. Furthermore, the constrained best fit parameters, see the lower portion of Table 3, are very similar to the best fit parameters. The details of the crystal field parameters, B_2^0 and B_2^2 , and the specific Hamiltonian used in the fits may be found in the *User Manual* provided with the PHI code.^{55,56} In the above fits, B_2^0 and B_2^2 are used when the crystal field Hamiltonian is written in a total spin-orbit basis in the operator equivalent formalism^{57,58} of Stevens. These parameters are not the usual zero-field splitting parameters, D and E , that apply when the magnetic moment is a spin-only moment. After correction for the cobalt(II) occupancies, the 5 K magnetization is virtually identical for compounds **2a** and **2b**, and the temperature dependencies of $\chi_{\text{M}}T$ are essentially the same between **2** and ca. 200 K. The small difference at the higher temperatures of ca. 0.1 emu K/mol, or ca. 2.5% at 300 K, is probably indicative of a temperature-dependent difference between the temperature of the sample and the temperature of the sensor, or a small error in the sample masses, or a small difference between the cobalt(II) occupancy in the single crystal, whose structure was determined, and the powder used for the magnetic studies, or even a small inhomogeneity in the cobalt(II) partial occupancy. At this point, it is simply not possible to determine which factor, or combination of factors, yields the small differences in $\chi_{\text{M}}T$ above 200 K. As expected, the axial linear **2a** and **2b** complexes do not require a nonzero value of B_2^2 . In contrast, the magnetic properties of **1** do require a nonzero B_2^2 value as a consequence of its pseudotetrahedral coordination environment about the cobalt(II) ion, see Figure 1. The remaining parameters of **1** are similar to those of **2a** and **2b** with the unexpected exception⁵⁹ of g_z being less than $g_x = g_y$. The fitted parameters given in the lower two portions of Table 3 are quite similar to those reported recently for the two-coordinate linear cobalt(II) complex, $\text{Co}[\text{N}(\text{SiMe}_3)\text{Dipp}]_2$ (Dipp = $\text{C}_6\text{H}_3\text{-2,6-Pr}_2^i$).²³ The $L = 2$ orbital contribution to the moment required to fit the $\chi_{\text{M}}T$ of **1**, **2a**, and **2b** indicates that the ordering of the cobalt(II) 3d orbitals is similar to the $d_z^2 < d_{xy} \sim d_{x^2-y^2} < d_{xz} \sim d_{yz}$ ordering obtained¹⁵ by *ab initio* calculations for the 3d⁷ electronic configuration of the two-coordinate linear iron(I) anionic complex, $[\text{Fe}\{\text{C}(\text{SiMe}_3)_3\}_2]^-$. In this case one of the three electrons in the virtually degenerate d_{xy} and $d_{x^2-y^2}$ orbitals yields an $L = 2$ orbital contribution to the magnetic moment of the linear complexes **2a** and **2b** and the pseudotetrahedral **1** complexes. The small g_z value of **1** seems to be an indication that $L = 1$ rather than 2, but when modeled, the fit of $\chi_{\text{M}}T$ required a very large $N\alpha$ value and yielded parameters that were unreasonable, even though the 5 K magnetization was well fitted with $L = 1$. At this time, it seems that the magnetic characterization differences in **1** versus **2a/2b** can be attributed mainly to their distinct geometries and their effects on the orbital magnetism.

CONCLUSIONS

In summary, we have structurally, magnetically, and spectroscopically characterized the first monomeric two-coordinate bis(aryloxy) cobalt species, $\text{Co}(\text{OAr}^{\text{Me}_6})_2$ (**1**) and $\text{Co}(\text{OAr}^{\text{iPr}_4})_2$ (**2a** and **2b**). Complexes **1**, **2a**, and **2b** are rare examples of two-coordinate transition metal(II) aryloxides, and

they are the first monomeric neutral linear and bent two-coordinate cobalt(II) aryloxy species to be characterized. Their structures refine with partially occupied cobalt(II) sites that result from the different steric effects of the ligands and the reaction conditions. In the analysis of the magnetic data, the bent and linear species may be described as paramagnetic complexes exhibiting large $\chi_{\text{M}}T$ values and corresponding effective magnetic moments that indicate strong spin-orbit coupling effects. A more detailed study is currently underway using an extensive series of compounds to further investigate the effects of steric and dispersion forces on the metal occupancies in these types of structures.

ASSOCIATED CONTENT

Supporting Information

CIFs for **1**, **2a**, and **2b**; UV-vis spectra of **1** and **2a**; IR spectra of **1**, **2a**, $\text{HOAr}^{\text{Me}_6}$, $\text{HOAr}^{\text{iPr}_4}$, and **2a** doped with excess $\text{HOAr}^{\text{iPr}_4}$. This material is available free of charge via the Internet at <http://pubs.acs.org>.

AUTHOR INFORMATION

Corresponding Author

*E-mail: pppower@ucdavis.edu (P.P.P.), glong@mst.edu (G.J.L.).

Notes

The authors declare no competing financial interest.

ACKNOWLEDGMENTS

This research was supported by National Science Foundation (NSF) (through Grant Nos. CHE-1263760 and DBIO 722538). A.M.B. thanks the NSF-Graduate Research Fellowship Program for their financial support (Grant No. DGE-1148897) and Professor M. M. Olmstead for her invaluable crystallographic support.

REFERENCES

- (1) Power, P. P. *Chem. Rev.* **2012**, *112*, 3482–3507.
- (2) Kays, D. L. *Dalton Trans.* **2011**, *40*, 769–778.
- (3) Power, P. P. *J. Organomet. Chem.* **2004**, *689*, 3904–3919.
- (4) Bryan, A. M.; Merrill, W. A.; Reiff, W. M.; Fettinger, J. C.; Power, P. P. *Inorg. Chem.* **2012**, *51*, 3366–3373.
- (5) Zadrozny, J. M.; Atanasov, M.; Bryan, A. M.; Lin, C.-Y.; Rekken, B. D.; Power, P. P.; Neese, F.; Long, J. R. *Chem. Sci.* **2013**, *4*, 125–138.
- (6) Reiff, W. M.; LaPointe, A. M.; Witten, E. H. *J. Am. Chem. Soc.* **2004**, *126*, 10206–10207.
- (7) Reiff, W. M.; Schulz, C. E.; Whangbo, M.-H.; Seo, J. I.; Lee, Y. S.; Potratz, G. R.; Spicer, C. W.; Girolami, G. S. *J. Am. Chem. Soc.* **2009**, *131*, 404–405.
- (8) Merrill, W. A.; Stich, T. A.; Brynda, M.; Yeagle, G. J.; Fettinger, J. C.; De Hont, R.; Reiff, W. M.; Schulz, C. E.; Britt, R. D.; Power, P. P. *J. Am. Chem. Soc.* **2009**, *131*, 12693–12702.
- (9) Layfield, R. A.; McDouall, J. J. W.; Scheer, M.; Schwarzmaier, C.; Tuna, F. *Chem. Commun.* **2011**, *47*, 10623–10625.
- (10) Ingleson, M. J.; Layfield, R. A. *Chem. Commun.* **2012**, *48*, 3579–3589.
- (11) Bradley, D. C.; Hursthouse, M. B.; Malik, K. M. A.; Mösele, R. *Transition Met. Chem.* **1978**, *3*, 253–254.
- (12) Murray, B. D.; Power, P. P. *Inorg. Chem.* **1984**, *23*, 4585–4588.
- (13) Sulway, S. A.; Collison, D.; McDouall, J. J. W.; Tuna, F.; Layfield, R. A. *Inorg. Chem.* **2011**, *50*, 2521–2526.
- (14) Neese, F.; Pantazis, D. A. *Faraday Discuss.* **2011**, *148*, 229–238.
- (15) Zadrozny, J. M.; Xiao, D. J.; Atanasov, M.; Long, G. J.; Grandjean, F.; Neese, F.; Long, J. R. *Nat. Chem.* **2013**, *5*, 577–581.
- (16) Boča, R. *Coord. Chem. Rev.* **2004**, *248*, 757–815.

- (17) Drago, R. S. *Physical Methods in Chemistry*; Saunders: Philadelphia, 1977; p 478.
- (18) Mannini, M.; Pineider, F.; Saintcavitt, P.; Danieli, C.; Otero, E.; Sciancalepore, C.; Talarico, A. M.; Arrio, M.-A.; Cornia, A.; Gatteschi, D.; Sessoli, R. *Nat. Mater.* **2009**, *8*, 194–197.
- (19) Leuenerberger, M. N.; Loss, D. *Nature* **2001**, *410*, 789–793.
- (20) Ardavan, A.; Rival, O.; Morton, J. J. L.; Blundell, S. J.; Tyryshkin, A. M.; Timco, G. A.; Winpenny, R. E. P. *Phys. Rev. Lett.* **2007**, *98*, 057201–057204.
- (21) Stamp, P. C. E.; Gaita-Ariño, A. *J. Mater. Chem.* **2009**, *19*, 1718–1730.
- (22) Boynton, J. N.; Guo, J.-D.; Fettinger, J. C.; Melton, C. E.; Nagase, S.; Power, P. P. *J. Am. Chem. Soc.* **2013**, *135*, 10720–10728.
- (23) Lin, C.-Y.; Guo, J.-D.; Fettinger, J. C.; Nagase, S.; Grandjean, F.; Long, G. J.; Chilton, N. F.; Power, P. P. *Inorg. Chem.* **2013**, *52*, 13584–13593.
- (24) Boynton, J. N.; Merrill, W. A.; Reiff, W. M.; Fettinger, J. C.; Power, P. P. *Inorg. Chem.* **2012**, *51*, 3212–3219.
- (25) Andersen, R. A.; Faegri, K.; Green, J. C.; Haaland, A.; Lappert, M. F.; Leung, W. P.; Rypdal, K. *Inorg. Chem.* **1988**, *27*, 1782–1786.
- (26) Li, J.; Song, H.; Cui, C.; Cheng, J. P. *Inorg. Chem.* **2008**, *47*, 3468–3470.
- (27) Andersen, R. A.; Haaland, A.; Rypdal, K.; Volden, H. V. *J. Chem. Soc., Chem. Commun.* **1985**, 1807–1808.
- (28) Andersen, R. A.; Carmona-Guzman, E.; Gibson, J. F.; Wilkinson, G. *J. Chem. Soc., Dalton Trans.* **1976**, 2204–2211.
- (29) Andersen, R. A.; Berg, D. J.; Fernholt, L.; Faegri, K.; Green, J. L.; Haaland, A.; Lappert, M. F.; Leung, W.-P.; Rypdal, K. *Acta Chem. Scand.* **1988**, *42a*, 554–562.
- (30) Buttrus, N. H.; Eaborn, C.; Hitchcock, P. B.; Sullivan, A. C. *J. Chem. Soc., Chem. Commun.* **1985**, 1380–1381.
- (31) Viehhaus, T.; Schwartz, W.; Hübler, K.; Locke, K.; Weidlein, J. Z. *Anorg. Allg. Chem.* **2001**, *627*, 715–725.
- (32) LaPointe, A. M. *Inorg. Chim. Acta* **2003**, *345*, 359–362.
- (33) Nguyen, T.; Panda, A.; Olmstead, M. M.; Richards, A. F.; Stender, M.; Brynda, M.; Power, P. P. *J. Am. Chem. Soc.* **2005**, *127*, 8545–8552.
- (34) Alberoli, A.; Blair, V. L.; Carrella, L. M.; Clegg, W.; Kennedy, A. R.; Klett, J.; Mulvey, R. E.; Newton, S.; Rentschler, E.; Russo, L. *Organometallics* **2009**, *28*, 2112–2118.
- (35) Kays, D. L.; Cowley, A. R. *Chem. Commun.* **2007**, 1053–1055.
- (36) Ni, C.; Fettinger, J. C.; Long, G. J.; Brynda, M.; Power, P. P. *Chem. Commun.* **2008**, *45*, 6045–6047.
- (37) Miyake, R.; Ishida, Y.; Kawaguchi, H. *J. Organomet. Chem.* **2011**, *696*, 4046–4050.
- (38) Olmstead, M. M.; Power, P. P.; Sigel, G. *Inorg. Chem.* **1986**, *25*, 1027–1033.
- (39) Yuan, C.; Xu, X.; Zhang, Y.; Ji, S. *Chin. J. Chem.* **2012**, *30*, 1474–1478.
- (40) Sigel, G. A.; Bartlett, R. A.; Decker, D.; Olmstead, M. M.; Power, P. P. *Inorg. Chem.* **1987**, *26*, 1773–1780.
- (41) Cantalupo, S. A.; Lum, J. S.; Buzzeo, M. C.; Moore, C.; DiPasquale, A. G.; Rheingold, A. L.; Doerrer, L. H. *Dalton Trans.* **2010**, *39*, 374–383.
- (42) Pangborn, A. B.; Giardello, M. A.; Grubbs, R. H.; Rosen, R. K.; Timmens, F. J. *Organometallics* **1996**, *15*, 1518–1520.
- (43) Dickie, D. A.; MacIntosh, I. S.; Ino, D. D.; He, Q.; Labeodan, O. A.; Jennings, M. C.; Schatte, G.; Walsby, C. J.; Clyburne, J. A. C. *Can. J. Chem.* **2008**, *86*, 20–31.
- (44) Stanciu, C.; Olmstead, M. M.; Phillips, A. D.; Stender, M.; Power, P. P. *Eur. J. Inorg. Chem.* **2003**, *18*, 3495–3500.
- (45) Bryan, A. M.; Long, G. J.; Grandjean, F.; Power, P. P. *Inorg. Chem.* **2013**, *52*, 12152–12160.
- (46) Hope, H. *Prog. Inorg. Chem.* **1995**, *41*, 1–19.
- (47) Sheldrick, G. M. *SADABS, Siemens Area Detector Absorption Correction*; Universität Göttingen: Göttingen, Germany, 2008.
- (48) Sheldrick, G. M. *SHELXTL-2013 and SHELXL-2013*; Universität Göttingen: Göttingen, Germany, 2013.
- (49) Dolomanov, O. V.; Bourhis, L. J.; Gildea, R. J.; Howard, J. A. K.; Puschmann, H. *Appl. Crystallogr.* **2009**, *42*, 339–341.
- (50) Bain, G. A.; Berry, J. F. *J. Chem. Educ.* **2008**, *85*, 532–536.
- (51) Chen, H.; Bartlett, R. A.; Dias, H. V. R.; Olmstead, M. M.; Power, P. P. *J. Am. Chem. Soc.* **1989**, *111*, 4338–4345.
- (52) (a) Rekken, B. D.; Brown, T. M.; Fettinger, J. C.; Tuononen, H. M.; Power, P. P. *J. Am. Chem. Soc.* **2012**, *134*, 6504–6507. (b) Rekken, B. D.; Brown, T. M.; Fettinger, J. C.; Lips, F.; Tuononen, H. M.; Herber, R. H.; Power, P. P. *J. Am. Chem. Soc.* **2013**, *135*, 10134–10148.
- (53) (a) Ndambuki, S.; Ziegler, T. *Inorg. Chem.* **2012**, *51*, 7794–7800. (b) Boynton, J. N.; Guo, J.-D.; Grandjean, F.; Fettinger, J. C.; Nagase, S.; Long, G. J.; Power, P. P. *Inorg. Chem.* **2013**, *52*, 14216–14223.
- (54) Ni, C.; Rekken, B.; Fettinger, J. C.; Long, G. J.; Power, P. P. *Dalton Trans.* **2009**, 8349–8355.
- (55) Chilton, N. F.; Anderson, R. P.; Turner, L. D.; Soncini, A.; Murray, K. S. *J. Comput. Chem.* **2013**, *34*, 1164–1175.
- (56) Chilton, N. F. *Phi User Manual v1.6*; 2011.
- (57) Bleaney, B.; Stevens, K. W. H. *Rep. Prog. Phys.* **1953**, *16*, 108–159.
- (58) Stevens, K. W. H. *Proc. Phys. Soc. A* **1952**, *65*, 209–215.
- (59) Kahn, O. *Molecular Magnetism*; VCH-Wiley: New York, 1993; p 12.